THE JOURNAL OF BIOLOGICAL CHEMISTRY VOL. 287, NO. 5, pp. 3337–3348, January 27, 2012


# Lectin Site Ligation of CR3 Induces Conformational Changes and Signaling*[S]

Received for publication, August 26, 2011, and in revised form, December 1, 2011 Published, JBC Papers in Press, December 9, 2011, DOI 10.1074/jbc.M111.298307

**Xian M. O'Brien[‡§1,2], Katie E. Heflin[‡§1], Liz M. Lavigne[‡], Kebing Yu[¶], Minsoo Kim[‖], Arthur R. Salomon[¶], and Jonathan S. Reichner[‡]**

*From the [‡]Division of Surgical Research, Department of Surgery, Rhode Island Hospital and the Warren Alpert Medical School of Brown University, Providence, Rhode Island 02903, the [§]Graduate Program in Pathobiology, Brown University, Providence, Rhode Island 02912, the [¶]Department of Molecular Biology, Cell Biology, and Biochemistry, Brown University, Providence, Rhode Island 02914, and the [‖]David H. Smith Center for Vaccine Biology and Immunology, Department of Microbiology and Immunology, University of Rochester, Rochester, New York 14642*

**Background:** CR3 is a $\beta_2$ integrin that contains a lectin-like domain that binds the fungal pathogen-associated molecular pattern $\beta$-glucan.
**Results:** Soluble $\beta$-glucan stabilizes an intermediate CR3 conformation that induces differential intracellular phosphorylation.
**Conclusion:** CR3 is a signaling pattern recognition receptor for $\beta$-glucan.
**Significance:** The CR3 receptor is a target for the design of novel immune modulators.

**Neutrophils provide an innate immune response to tissues infected with fungal pathogens such as *Candida albicans*. This response is tightly regulated in part through the interaction of integrins with extracellular matrix ligands that are distributed within infected tissues. The $\beta_2$ integrin, CR3 (CD11b/CD18), is unique among integrins in containing a lectin-like domain that binds the fungal pathogen-associated molecular pattern $\beta$-glucan and serves as the dominant receptor for recognition of fungal pathogens by human granulocytes. $\beta$-Glucan, when isolated in soluble form, has been shown to be a safe and effective immune potentiator when administered therapeutically. Currently a pharmaceutical grade preparation of $\beta$-glucan is in several clinical trials with an anti-cancer indication. CR3 binding of extracellular matrix, carbohydrate, or both ligands simultaneously differentially regulates neutrophil function through a mechanism not clearly understood. Using FRET reporters, we interrogated the effects of soluble $\beta$-glucan on intracellular and extracellular CR3 structure. Although the canonical CR3 ligand fibrinogen induced full activation, $\beta$-glucan alone or in conjunction with fibrinogen stabilized an intermediate conformation with moderate headpiece extension and full cytoplasmic tail separation. A set of phosphopeptides differentially regulated by $\beta$-glucan in a CR3-dependent manner were identified using functional proteomics and found to be enriched for signaling molecules and proteins involved in transcriptional regulation, mRNA processing, and alternative splicing. These data confirm that CR3 is a signaling pattern recognition receptor for $\beta$-glucan and represent the first direct evidence of soluble $\beta$-glucan binding and affecting a signaling-competent intermediate CR3 conformation on living cells.**

Neutrophils act as the body's first cellular line of defense, responding to injury or infection by quickly migrating from the vasculature to a site of tissue damage, in part through the coordinated regulation of surface integrins. The leukocyte integrin CR3[3] (CD11b/CD18) is unique among integrins in that it has two distinct ligand-binding sites. The I-domain binds canonical ligands including extracellular matrix proteins, the complement component iC3b, and intercellular adhesion molecules such as intercellular adhesion molecule 1 (ICAM-1). CR3 also contains a carbohydrate binding lectin-like domain C-terminal to the I-domain that can bind $\beta$-glucan, a (1,3)(1,6)-$\beta$-D-linked glucose polymer, found normally as a structural component of fungal cell walls and which functions as a fungal pathogen-associated molecular pattern (PAMP) (see Fig. 1*A*) (1–3). Studies have shown that leukocyte function is differentially regulated upon ligation of CR3 at the I-domain, the lectin site, or both together (4–6). It is not known whether these functional differences reflect distinct mechanisms of activation upon ligation at its two binding sites.

In addition to encountering $\beta$-glucan within the cell wall of intact fungi, it is known that patients with deep-seated mycotic infections elaborate soluble $\beta$-glucan (s$\beta$glu) as a breakdown product from the fungal cell surface that may be present surrounding the foci of infection and immobilized within the matrix of infected tissues (7). In this way, s$\beta$glu is thought to extend its immunomodulatory effect as a fungal PAMP to peripheral blood leukocytes. A purified form of s$\beta$glu has been

* This work was supported, in whole or in part, by National Institutes of Health Grants GM-066194 and AI-079582 (to J. S. R.). This work was also supported by Grant Assistance in Areas of National Need from the United States Department of Education (to X. M. O.) and allocations to the Department of Surgery by Rhode Island Hospital.
[S] This article contains supplemental Figs. S1–S3 and Tables S1 and S2.
[1] Both authors contributed equally to this manuscript.
[2] To whom correspondence should be addressed: Dept. of Surgery, Rhode Island Hospital, 593 Eddy St., Providence, RI 02903. Tel.: 401-439-8206; Fax: 401-444-8052; E-mail address: xianobrien@gmail.com.

[3] The abbreviations used are: CR3, CD11b/CD18; CFP, cyan fluorescent protein; dPBS, Dulbecco's PBS; Fgn, fibrinogen; FgnD, Fgn fragment D; fMLP, bacterial *n*-formyl peptide (formylmethionylleucylphenylalanine); L-15, Leibovitz L15 medium; mCFP, monomeric cyan fluorescent protein; mYFP, monomeric yellow fluorescent protein; ORB, octadecyl rhodamine B; PAMP, pathogen-associated molecular pattern; s$\beta$glu, soluble $\beta$-glucan; SILAC, stable isotope labeling with amino acids in cell culture.

developed for immune priming with anti-infectious and anti-cancer indications that are being explored clinically (8–12). Whether released from a fungal burden or administered therapeutically, sβglu has been shown to influence the functional phenotype of neutrophils through changes in migration, adhesion, and respiratory burst (3, 4, 13).

How cells are able to discriminate the context of β-glucan presentation to provide the appropriate cellular response to direct contact with the intact pathogen (*e.g.* phagocytosis and production of reactive oxygen species) or to induce a primed state, inflammatory response, or changes in migration that are more suited to activation at a distance by soluble mediators is a topic of active research. Several distinct mammalian receptors for β-glucan have been identified in addition to CR3: Dectin-1, lactosylceraminde. and scavenger receptors (14–17); however, it is still unclear how each receptor distinguishes its ligand. Goodridge *et al.* (18) have recently shown that although Dectin-1 can bind both soluble and particulate β-glucan, signaling is only activated by particulate β-glucans, positing a "phagocytic synapse" that allows discrimination of direct microbial contact from soluble mediators. These findings underscore a possible mechanistic niche for CR3 that shows distinct functional responses to both immobilized and soluble β-glucan (3, 4, 12, 13, 19–21). Although functional evidence has been used to argue for CR3 as a receptor for β-glucan, there has been no direct evidence of β-glucan inducing a change in CR3 conformation at a physiochemical or structural level. In this study we investigate whether CR3 functions as a signaling receptor in response to sβglu.

Integrins have long been thought to undergo conformational rearrangements upon activation speculated to correlate with increased ligand binding and initiation of intracellular signaling (22). The studies herein use FRET to investigate changes in the spatial separation of the α and β cytoplasmic domains and extracellular conformational changes of CR3 upon differential activation of the I-domain or the lectin-like site. The use of FRET is unique in that it allows highly sensitive changes in integrin activity to be measured in viable cells in real time. We have exploited this tool to investigate changes in conformation of both the intracellular and extracellular regions of CR3 in response to the I-domain ligand, fibrinogen (Fgn), and the lectin-like domain ligand, sβglu. To extend our investigation we also employed a functional proteomics approach using isogenic K562 cells that differ only in their expression of CR3 to identify phosphopeptides that are modulated in response to sβglu. These K562-derived cell lines allow a specific interrogation of the CR3-dependent processes and, unlike primary neutrophils, can be propagated in culture to facilitate an MS-coupled technique called stable isotope labeling with amino acids in cell culture (SILAC). The resultant phosphopeptide signature represents the first global demonstration of CR3-dependent signaling in response to sβglu. This along with the associated conformational changes in intracellular and extracellular domains of CR3 may represent the β-glucan initiated primed state.

## EXPERIMENTAL PROCEDURES

*Reagents*—RPMI 1640 Glutamax, Dulbecco's PBS (dPBS), Hanks' balanced salt solution, Leibovitz L-15 medium (L-15), anti-CD11b (ICRF44), and anti-CD11b (Mo-1) were from Invitrogen. MEM 199 was from Cambrex (East Rutherford, NJ). FBS was from Atlanta Biologicals (Atlanta, GA). Normocin was from Lonza (Basil, Switzerland). Highly purified, soluble yeast β-glucan (ImPrime PGG™), whole glucan particles, and anti-glucan monoclonal antibody (mAb) (clone BFDiv) were provided by Biothera (Eagan, MN). The β-glucan preparation contained <0.02% protein, <0.01% mannan, and 1% glucosamine. Human fibrinogen fragment D (FgnD) was from EMD (San Diego, CA). Anti-CD11b (LM2/1) was from Bender Medical Systems (Vienna, Austria). FITC-conjugated human fibrinogen was from Molecular Innovations (Novi, MN). FITC-conjugated anti-CD11b (CBRM1/5) was from BioLegend (San Diego, CA). FITC-conjugated mouse IgG1 (679.1Mc7) was from Beckman Coulter (Brea, CA). FITC-conjugated anti-CD11b (ICRF44) was from Ancell (Bayport, MN). All other reagents were the highest grade available and were from Sigma unless otherwise noted.

*Neutrophil Preparation*—With Rhode Island Hospital Institutional Review Board oversight and approval, neutrophils were isolated from healthy human volunteers into EDTA-containing Vacutainer tubes (BD Biosciences). Histopaque cell separation was followed by gravity sedimentation through 3% dextran. Hypotonic lysis to remove erythrocytes yielded a neutrophil purity of >95%. Neutrophils were suspended in Hanks' balanced salt solution (without $Ca^{2+}$/$Mg^{2+}$) on ice until use. All reagents contained <0.1pg/ml endotoxin.

*Immunofluorescence of Neutrophil-Hyphae Interaction*—Delta T dishes (Bioptechs, Butler, PA) were coated with 50 μg/ml fibronectin in TBS, pH 9, overnight at 37 °C. An overnight culture of *Candida albicans* was washed twice, and 1 ml of $1 \times 10^5$/ml cells in MEM 199 was added to dishes and grown into hyphae overnight at 37 °C. BSA was added to a concentration of 100 μg/ml and incubated at room temperature 1 h. MEM 199 was aspirated and replaced with 25,000 neutrophils in 1 ml of L-15, incubated for 45 min at 37 °C, and formaldehyde-fixed. Cells were rinsed, blocked with 10% Fc block (BD Bioscience) and 10% FBS in dPBS, then incubated for 60 min with 10% Fc block, 1% FBS and a mixture of ICRF44 (1:20), LM2/1 (1:20), Mo-1 (1:20), and BFDiv (1:50). Cells were washed twice and incubated for 30 min with Texas Red anti-mouse IgG $F(ab')_2$ (1:50) plus FITC anti-mouse IgM (1:50) in dPBS with 1% serum, washed 3 times with dPBS, and imaged.

*Cell Culture and Transfection*—K562 cell line was from ATCC (Manassas, VA). K562-CR3 stable cell line was established as described (23). The K562 cell line stably expressing a FRET construct reporting the separation of the cytoplasmic tails of integrin LFA1 (designated in this work as K562:LFA1-FRETa) was established as described (24). K562 cells were cultured in RPMI 1640 Glutamax with 1% Normocin and 10% FBS. Puromycin or G418 were used where needed for selection.

For SILAC studies, K562 cells and K562-CR3 cells were cultured in arginine- and lysine-deficient RPMI 1640 medium (Fisher) supplemented with 13C6, 15N4 arginine and 13C6, 15N2 lysine (Cambridge Isotope Laboratories, Andover, MA), 10% heat-inactivated dialyzed FBS, and 1% Normocin.

*Plasmid Construction*—Generation of $\beta_2$-monomeric yellow fluorescent protein (mYFP) constructs was previously de-

scribed (24). An $\alpha_M$ monomeric cyan fluorescent protein (mCFP) fusion construct with a linker sequence of APEPAPRPTAAPEPAKRARDPPVAT was generated as described in the supplemental Experimental Procedures.

*Generation of K562:CR3-FRETa Stable Cell Line*—K562 cells co-transfected with $\alpha_M$(25)mCFP, consisting of the $\alpha_M$ chain linked to a monomeric CFP by a 25-amino acid linker, and $\beta_2$(12)mYFP, consisting of the $\beta_2$ chain linked to monomeric YFP by a 12-amino acid linker (described in supplemental Fig. S1*A*) were propagated under selective antibiotic pressure and underwent two rounds of selective enrichment by FACS. Putative clones were single-sorted into 96-well dishes, expanded, and characterized for FRET response and protein expression. From these, a stable line, K562:CR3-FRETa, was established and verified by Western blot (supplemental Fig. S1*C*), PCR, and sequence analysis. Both the reporter construct and stable line have competent receptor function (supplemental Figs. S1*D* and S2).

*Cell Preparation and Activation for Cytoplasmic Tail FRET*—$2.5 \times 10^5$ K562:CR3-FRETa cells or K562:LFA1-FRETa were washed and resuspended in a 0.75–1 ml of L-15 supplemented with 2 mg/ml D-glucose. Cells were treated in heatable glass-bottom Delta T dishes or 15-ml tubes for analysis as 30 μl drops on coverglass. Cells were treated at 37 °C for 15 min in L-15 supplemented with 2 mg/ml D-glucose with or without 1 mM $Mn^{2+}$. Treatment was in the presence of 1% human serum where indicated. I-domain ligand binding conditions were 25 μg/ml FgnD or 50 μg/ml full-length human Fgn. 20 nM phorbol 12-myristate 13-acetate or 50 μg/ml sβglu was supplemented where noted.

*Microscopy and Cytoplasmic Tail FRET Analysis*—Imaging was conducted on a Nikon Eclipse TE2000-U epifluorescence microscope (Tokyo, Japan) coupled to a CoolSNAP HQ CCD camera (Roper Scientific, Tucson, AZ) or iXon$^{EM}$ + 897E back-illuminated EMCCD camera (Andor, Belfast, UK) with a Bioptechs stage heater. Nikon CFP HQ, YFP HQ, and YFP BLEACH filter cubes without emission filters were used for CFP imaging, YFP imaging, and YFP bleaching. A xenon lamp illuminated cells through a 33-mm neutral density 4 (ND4) filter, and they were viewed through a 60× oil immersion Plan APO objective lens. Exposure time was 500 ms for both CFP and YFP. Acceptor photobleaching was done for 3.5 min without an ND filter using the YFP BLEACH cube. For each field pre- and post-bleach images of CFP and YFP were acquired. Image acquisition, registration, background subtraction, and data analysis were performed using NIS Elements (Nikon) and Excel (Microsoft, Seattle, WA) computational software.

Cells with similar CFP and YFP intensities were selected. After registration and background subtraction, the CFP signal in the cell membrane was masked as a region of interest for analysis. FRET efficiency ($E$) was calculated as $E = 1 - (F_{CFP(Pre)}/F_{CFP(Post)})$ (25), where $F_{CFP(Pre)}$ and $F_{CFP(Post)}$ are the mean CFP emission intensity before and after YFP photobleaching (24).

*FACS-based FRET Assay for Extracellular Extension of CR3*—Experiments were performed as described (23) and expanded in supplemental Experimental Procedures. Briefly, neutrophils were suspended at $1 \times 10^7$ cells/ml in BSS+ buffer (0.1% BSA, 1 mM $CaCl_2$, 1 mM $MgCl_2$) with 10% donor serum. Cells were stimulated with 10 nM bacterial *n*-formyl peptide (fMLP), 25 μg/ml FgnD, 50 μg/ml sβglu, or combinations for 15 min at 37 °C, and 100-μl cell aliquots were incubated with FITC-IgG control (10 μg/ml), FITC-ICRF44 (9.8 μg/ml), or FITC-CBRM1/5 (15 μg/ml) for 60 min with rotation at 4 °C in foil. Where indicated, cells were incubated with 200 μg/ml FITC-Fgn for 15 min at room temperature. Cells were washed 3 times with BSS+ at 4 °C and split into four 125-μl aliquots in FACS-compatible snap cap tubes on ice. Octadecylrhodamine B (ORB) was added to a final volume of 250 μl and concentrations of 0, 75, 200, and 400 nM. Samples were incubated on ice for 20 min and analyzed by the Brown University Flow Cytometry and Sorting Facility on a BD FACSAria.

*SILAC*—SILAC is detailed in the supplemental Experimental Procedures. Briefly, $1 \times 10^7$ K562 or K562-CR3 cells were collected after at least seven doublings in SILAC media, washed twice, and resuspended in 1 ml of L-15 supplemented with 2 mg/ml D-glucose and 10% human serum. 100 μg/ml sβglu was added to the treatment tubes. Cells were incubated at 37 °C for 30 min, placed on ice, and washed twice with ice-cold dPBS, and aspirated pellets were frozen at −80 °C. Eight peptide samples were generated by combing cell types, SILAC label, and treatment conditions. Phosphopeptides were $TiO_2$-enriched, analyzed using automated nano-LC/ESI-MS, and processed using the High-throughput Autonomous Proteomic Pipeline platform. A list of phosphopeptides that changed significantly in K562-CR3 sβglu treatment *versus* K562-CR3 control but were unchanged in K562 sβglu treatment *versus* K562 control was identified (supplemental Table S1) as well as a list that changed significantly in K562-CR3 sβglu treatment *versus* K562 sβglu treatment but was unchanged in K562-CR3 control *versus* K562 control (supplemental Table S2).

*Statistics*—For SILAC experiments, $q$-values were calculated using R (R Foundation for Statistical Computing, Vienna, Austria), and significance was set at a $q < 0.1$. All other data were analyzed by Student's $t$ test or analysis of variance with post hoc Newman-Keuls as appropriate using Excel and MATLAB computational software. Values of $p < 0.01$ were considered statistically significant.

## RESULTS

*Neutrophil CR3 Colocalizes with Exposed β-Glucan on Live Yeast Hyphae*—Previous data from our laboratory (3, 20) have shown using both functional and antibody blocking studies that CR3 recognizes the fungal PAMP β-glucan on intact hyphae. An experiment was designed to demonstrate physical colocalization of CR3 with exposed β-glucan of live yeast hyphae in which neutrophils were added to established yeast hyphae. Cells were then fixed and stained for CR3 (*red*) and β-glucan (*green*). In areas of neutrophil-hyphae interaction, fluorescent microscopy reveals specific colocalization of CR3 to areas of exposed β-glucan (*yellow*), shown in Fig. 1*B*. These data support our model that CR3 acts as a pattern recognition receptor in the interaction of neutrophils with intact hyphae. It is known that sβglu is elaborated as a breakdown product from the fungal cell surface and may be present in the blood stream and tissue surrounding the primary site of infection (7). How sβglu primes

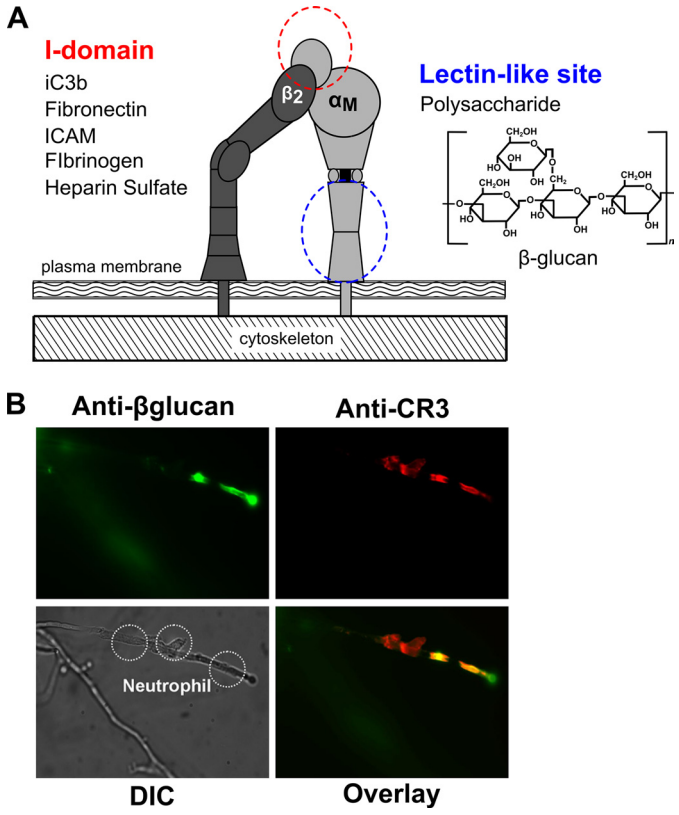


FIGURE 1. **CR3 binds extracellular matrix components and yeast β-glucan.** *A*, shown is a schematic of CR3 and representative binding sites within CR3 that permit dual occupancy of protein ligands in the I-domain and β-glucan in the lectin site. *ICAM*, intercellular adhesion molecule. *B*, shown is *in vitro* staining of β-glucan (FITC, *top left*) on live yeast hyphae interacting with neutrophils stained for CR3 (Texas Red, *top right*). The merged image indicates colocalization of CR3 to areas with immuno-accessible β-glucan in *yellow* (*bottom right*). Shown is a differential interference contrast (*DIC*) image (*bottom left*). FITC, Texas Red, and differential interference contrast images were acquired with a Nikon Eclipse TE2000-U epifluorescence microscope coupled to a CoolSNAP HQ CCD camera using NIS elements software. Nikon B-2E/C and Y-2E/C cubes were used for FITC and Texas Red imaging, respectively. Cells were visualized at 37 °C in L-15 medium with 2 mg/ml glucose. A xenon lamp was used to illuminate the cells that were viewed through a 40× Plan APO objective lens.

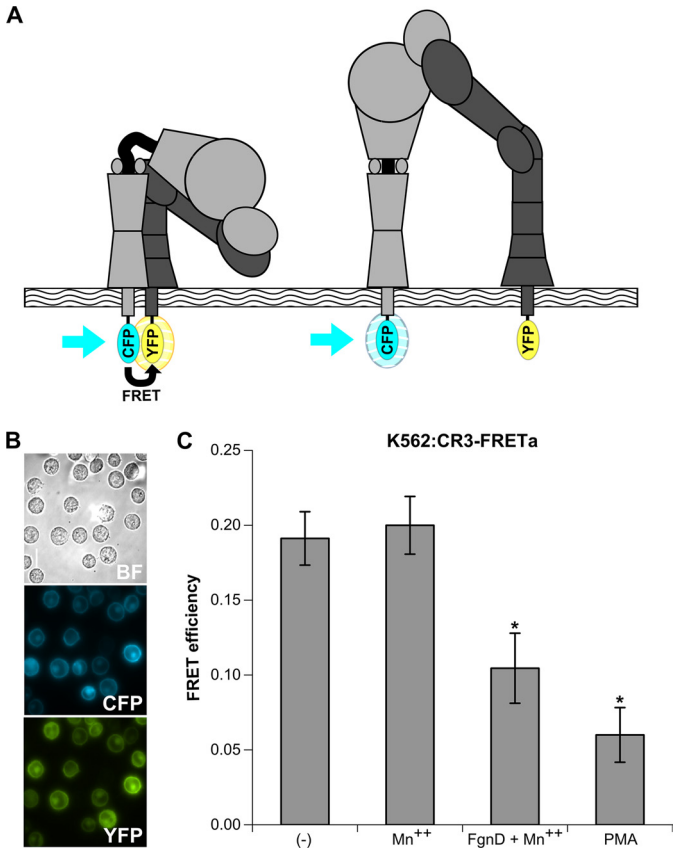


FIGURE 2. **The use of FRET to report integrin activation; development of a K562 cell line that stably expresses the CR3-FRET activation reporter; loss of FRET in activation reporter with native ligand.** *A*, the integrin activation FRET reporter is shown. In the inactive, bent conformation (*left*), the cytoplasmic domains of the α and β subunits are closely apposed, allowing for efficient FRET between mCFP and mYFP fused to these C termini. In the active, extended conformation (*right*), the α and β subunits lose their interactions in the tailpiece leading to a separation greater than 100 Å between the mCFP and mYFP, thereby abolishing FRET. See also supplemental Figs. S1 and S2 for reporter construction and functional characterization. *B*, shown are bright field (*BF*), CFP, and YFP images of the K562 cell line stably expressing the CR3-FRET activation construct (K562:CR3-FRETa) acquired with a Nikon Eclipse TE2000-U epifluorescence microscope coupled to a CoolSNAP HQ CCD camera using NIS elements software. Nikon CFP HQ and YFP HQ cubes without emission filters were used for CFP and YFP imaging, respectively. Cells were visualized at 37 °C in L-15 medium with 2 mg/ml glucose. A xenon lamp was used to illuminate the cells through a 33-mm ND4 filter, and the cells were viewed through a 60× oil immersion Plan APO objective lens. Exposure time was 500 ms for both CFP and YFP. *C*, FRET efficiencies: basal FRET, non-activating treatment with 1 mM $Mn^{2+}$ FRET, activation with 1 mM $Mn^{2+}$ plus 25 μg/ml FgnD or 20 nM phorbol 12-myristate 13-acetate (*PMA*). Each sample represents analysis of at least 25 cells in three separate experiments. *, $p < 0.01$.

peripheral blood leukocytes and signaling in response to sβglu is poorly characterized. To investigate this, a series of experiments was designed to determine if CR3 functions as a signaling receptor in response to sβglu.

*Generation of K562 Cell Line Stably Expressing CR3-FRET Activation Reporter*—Current mechanistic thought on the unique bidirectional signal transduction of integrins speculates that conformational rearrangements correlate with activation, increased ligand binding, and intracellular signaling (25). Kim *et al.* (24) provided compelling evidence for this hypothesis using a series of FRET reporters for the integrin LFA-1, suggesting that this bidirectional signal transduction is achieved through coupling the spatial separation of the α and β cytoplasmic domains with extracellular conformational change (24). The functional consequences and whether this manner of regulation is shared among integrins is a subject of current investigation. To that end we developed a FRET sensor to report the separation of CR3 cytoplasmic tails, allowing the measurement of integrin activation and ligand binding directly in living cells (Figs. 2*A* and supplemental Fig. S1). From this construct a stable line, K562:CR3-FRETa, was established (Fig. 2). Both the reporter construct and stable line have competent receptor function shown by both adhesion (supplemental Fig. S1*D*) and the ability to agglutinate with either iC3b-coated whole glucan particles or unicellular *C. albicans* (supplemental Fig. S2). Fig. 2 characterizes the FRET response of K562:CR3-FRETa. FRET in both untreated and $Mn^{2+}$-treated cells is significantly reduced upon binding Fgn or FgnD, which contains the CR3 I domain binding P2 motif of Fgn (27), or phorbol 12-myristate 13-acetate. The generation of this stable line eliminates some of the variability of transfection efficiency and surface expression levels.

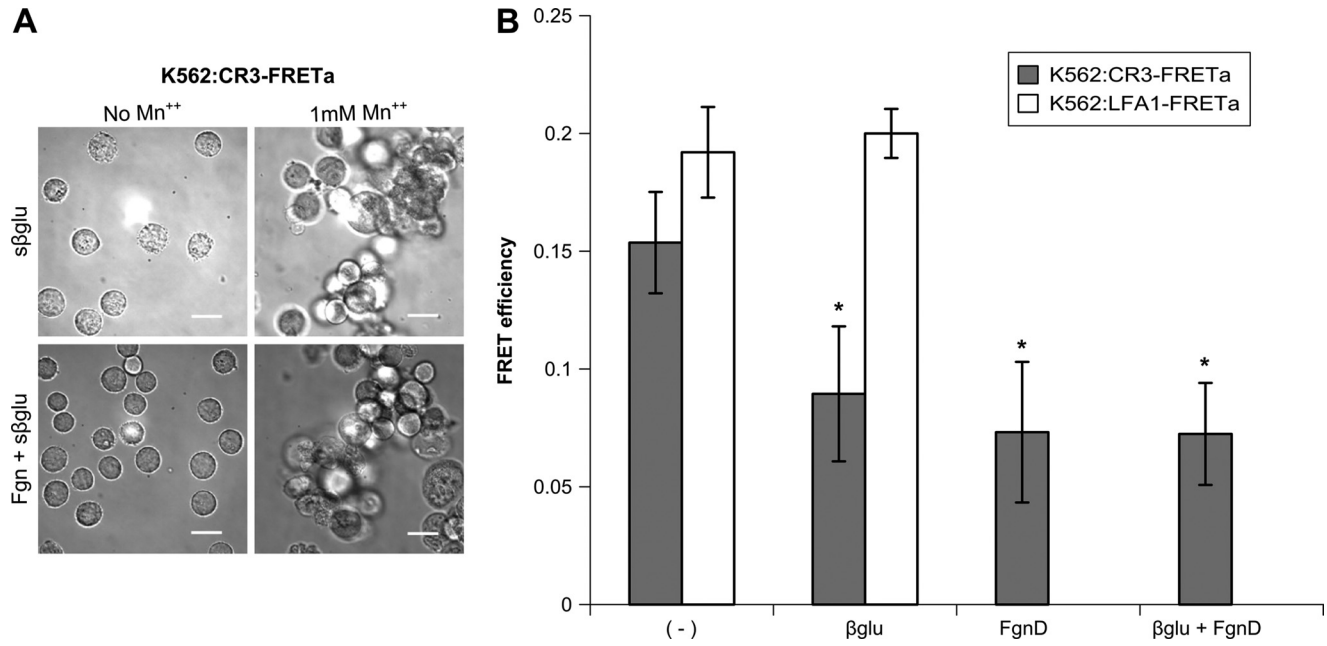


FIGURE 3. **Soluble β-glucan increases homotypic CR3 interactions and induces CR3 activation.** *A*, K562:CR3-FRETa were incubated with 50 μg/ml sβglu plus or minus 1 mM $Mn^{2+}$ in the presence or absence of 25 μg/ml FgnD. Large clumps, likely due to homotypic interactions, rendered FRET analysis difficult. Bright field images were acquired for each condition with a Nikon Eclipse TE2000-U epifluorescence microscope coupled to a CoolSNAP HQ CCD camera using NIS Elements software. Cells were visualized at 37 °C in L-15 medium with 2 mg/ml glucose. A xenon lamp was used to illuminate the cells through a 33-mm ND4 filter, and the cells were viewed through a 20× Plan APO objective lens. See also supplemental Figs. S1 and S2 for reporter construction and functional characterization. *B*, shown is the graphic comparison of FRET efficiencies of K562:CR3-FRETa (*gray bars*) and K562:LFA1-FRETa (*white bars*) for each treatment, performed in the presence of human serum and in the absence of $Mn^{2+}$. *, $p < 0.01$ *versus* untreated.

*β-Glucan Increases Homotypic CR3 Interactions and Specifically Induces Separation of CR3 Cytoplasmic Tails*—K562:CR3-FRETa cells were treated with sβglu plus or minus $Mn^{2+}$ in the presence or absence of FgnD. These cells formed large clumps in the presence of sβglu and $Mn^{2+}$, likely due to an increase in homotypic interactions, rendering FRET analysis difficult (Fig. 3*A*). K562:LFA1-FRETa cells, which express a FRET construct reporting the cytoplasmic tail separation of the β2 integrin LFA1, which lacks the lectin-like domain of CR3, were similarly treated but did not show homotypic aggregation (data not shown). As $Mn^{2+}$ facilitates activation but is not a requirement for integrin function, we performed our analysis in its absence. As shown in Fig. 3*B*, FRET is significantly reduced in the CR3-FRETa cells upon treatment with sβglu. LFA1-FRETa cells lacking the lectin-like domain showed no separation of cytoplasmic tails in response to sβglu treatment. Activation with FgnD or treatment with sβglu and FgnD also significantly reduced FRET in the CR3-FRETa cells, but no additive effect was observed. This separation of cytoplasmic tails suggests a mechanism by which sβglu may exert some of its immune priming effect. Experiments were conducted in the presence of human serum, but the observed cytoplasmic activation of CR3 was serum-independent for the treatments described here. Studies in the absence of serum or in the presence of heat-inactivated human serum showed no differences from the data reported in Fig. 3*B* (data not shown).

*sβglu Treatment of Human Neutrophils Reveals Activation-specific Epitope of CR3*—Previously published functional experiments suggest that sβglu does not fully activate cells. Although the CR3 FRET experiments shown above suggest that CR3 is activated by treatment with sβglu, those experiments only reveal the intracellular conformation of the receptor. To investigate the extracellular conformation of CR3 after treatment with sβglu, FACS experiments were performed on primary human neutrophils.

Cells were treated with either fMLP, FgnD, sβglu, or a combination of FgnD and sβglu in the presence of donor serum. Treated and control cells were labeled with FITC-ICRF44 (which binds to both inactive and extended conformations of CR3) (28), FITC-CBRM1/5 (which binds to an epitope revealed upon activation and extension), or FITC-Fgn (fibrinogen, a CR3 I-domain ligand, labeled with FITC) (Fig. 4*A*). fMLP treatment is known to enhance surface expression of CR3 as well as activating CR3, revealing the CBRM1/5-specific epitope (29). As shown in Fig. 4, *B–D*, with sβglu treatment we also see significant enhancement of the surface expression of CR3 (126 ± 18%), the exposure of the activation-specific epitope (138 ± 18%), and binding of FITC-labeled Fgn (126 ± 9%) but to a much lower extent to that seen with fMLP stimulation, which showed a significant increase of 206 ± 37, 250 ± 40, and 226 ± 29%, respectively. Neutrophils treated with unlabeled FgnD had significantly lower levels of ICRF44, both alone (67 ± 1%) or with sβglu (72 ± 3%), indicating CR3 internalization after binding. To specifically isolate the conformational dynamics of ligand bound CR3 on the cell surface, subsequent experiments used FITC-labeled fibrinogen (FITC-Fgn) as both a ligand and FRET reporter.

*sβglu Causes Small Magnitude of Extension of CR3 Extracellular Domain*—Because it is unclear at what point in the extension of activated CR3 the CBRM1/5 epitope becomes accessible, this leaves at least two possible ways of interpreting these results. The data could indicate that sβglu treatment causes a

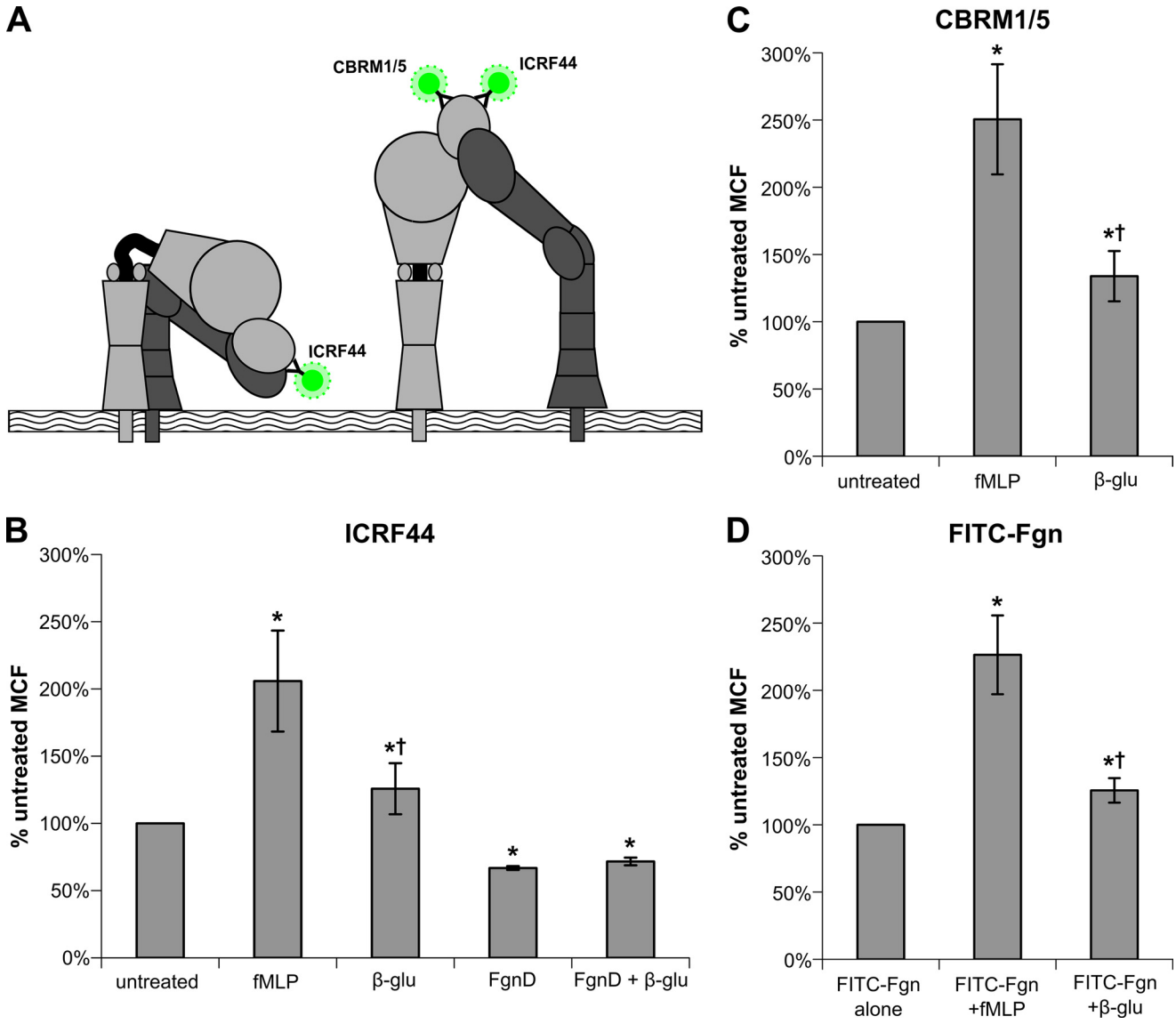


FIGURE 4. **Measuring exposure of an activation-specific epitope of CR3 in response to stimulation.** *A*, shown is a schematic indicating epitope binding of specific mAbs on inactive and fully extended CR3. *B*, freshly isolated neutrophils in the presence of donor serum were treated with either 10 nM fMLP, 25 μg/ml FgnD, 50 μg/ml sβglu, or combinations for 15 min. Treated and control cells were labeled with FITC-ICRF44 (which binds to both inactive and extended conformations of CR3) FITC-CBRM1/5 (which binds to an epitope revealed upon activation and extension) (*C*) or FITC-Fgn (a CR3 I-domain ligand) (*D*). Data are plotted as the fraction of FITC mean channel fluorescence (*MCF*) in untreated neutrophils and are from at least four independent experiments and blood donors, with each condition run in duplicate. *, $p < 0.01$ *versus* untreated; †, $p < 0.01$ 10 mM fMLP *versus* 50 μg/ml sβglu.

fewer CR3 molecules to become fully active than treatment with fMLP or that treatment with sβglu stabilizes the receptor into an intermediate conformation. To investigate these possibilities, a novel FRET-based system developed by Lefort *et al.* (23) was employed that allowed examination of conformational changes in the extracellular domain of CR3.

This FACS-based assay reports the relative distance between a FITC-labeled mAb or a FITC-labeled protein and ORB, a membrane partitioning fluorophore. Neutrophils labeled with ORB and FITC-conjugated mAb or protein are assayed using flow cytometry. Transfer of energy from the FITC donor to the ORB acceptor causes a decrease in the fluorescence intensity measured in the FITC channel that we plot as the ratio of FITC mean fluorescence intensity in the absence of ORB acceptor ($F_D$) to that in the presence of ORB acceptor ($F_{DA}$) *versus* ORB mean fluorescence (Fig. 5*A*). The slope of these lines quantitatively represents the extent of energy transfer from the donor to the acceptor. Conditions are compared by calculating a distance ratio ($L_2/L_1 = (S_1/S_2)^{1/4}$) that represents the change in donor-acceptor separation, where $L$ represents the distance of the donor fluorophore from the acceptor fluorophore in the cell membrane, and $S$ is the slope as calculated above. Using FITC-ICRF44 and FITC-CBRM1/5, we see a significantly greater distance ratio for FITC-CBRM1/5 (1.46 ± 0.11) than FITC-ICRF44 (1.25 ± 0.04) with fMLP that is consistent with previous data (23) (Fig. 5*E*). See Fig. 5, *B–D*, for representative data plots used to determine slope to calculate distance ratios. FITC-IgG isotype control confirmed the specificity of signal (data not shown).

As the active conformation of CR3 is thought to extend its headpiece a distance greater than 200 nm from the cell membrane where FRET would not be possible, the fact that greater

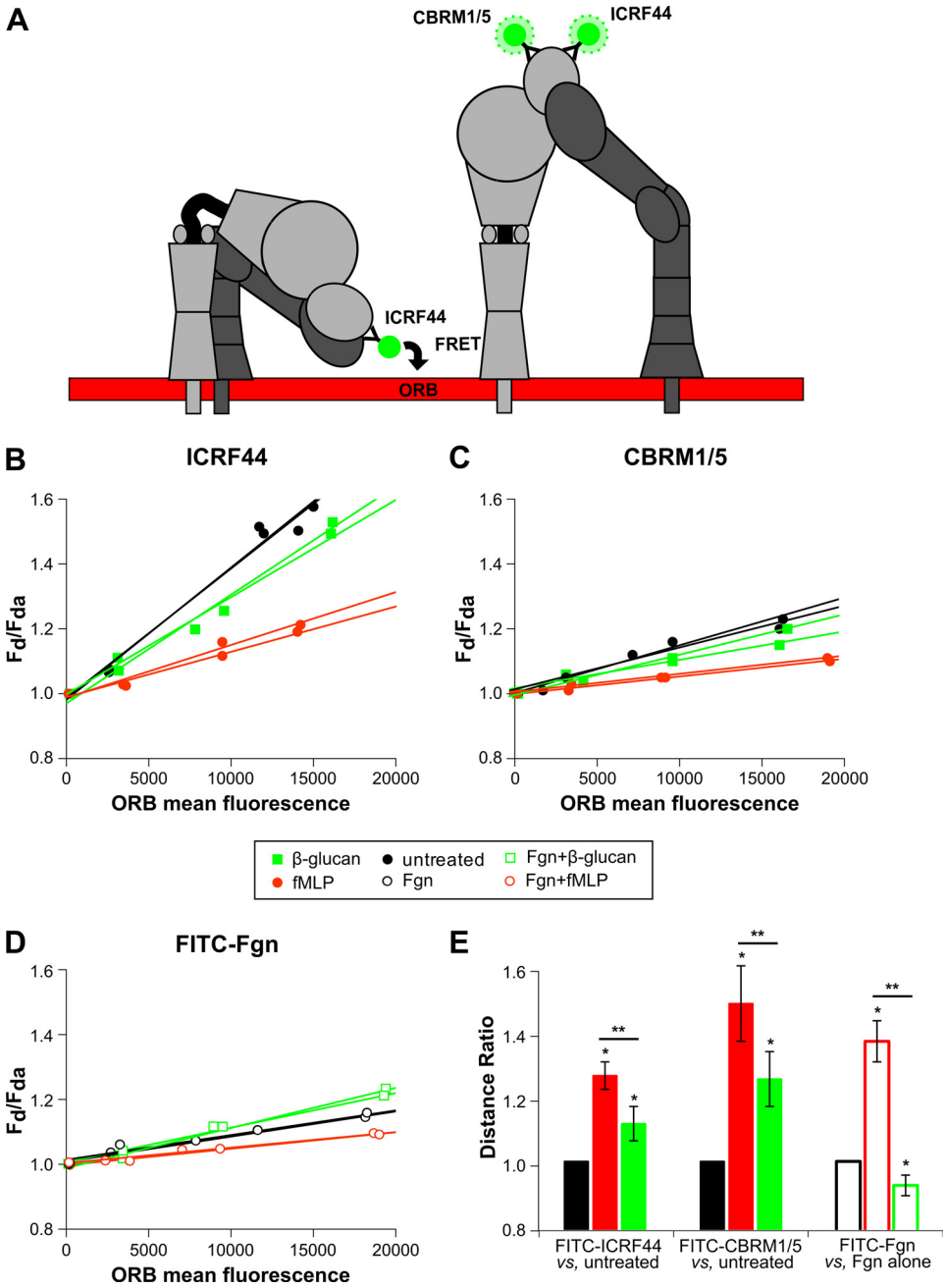


FIGURE 5. **Measuring extension of the extracellular domain of CR3 by loss of FRET in response to stimulation.** *A*, shown is a schematic demonstrating the loss of FRET between ORB membrane dye and FITC-conjugated mAbs upon the extension of the extracellular domain. *B–D*, freshly isolated neutrophils in the presence of donor serum were treated with either 10 nM fMLP or 50 μg/ml sβglu for 15 min. Treated and control cells were labeled with FITC-ICRF44 (*B*), FITC-CBRM1/5 (*C*), or FITC-Fgn (*D*). Neutrophils were then incubated with 0, 75, 200, or 400 nM ORB and then analyzed by FACS. Representative data are plotted as the fraction of donor mean fluorescence intensity in the absence of acceptor fluorophore ($F_D$) to that in the presence of acceptor fluorophore ($F_{DA}$) on the *y* axis ($F_D/F_{DA}$) *versus* ORB mean fluorescence on the *x* axis to normalize for CR3 expression levels. Plots represent a single blood donor, with duplicate samples for each condition. *E*, the slope of each line is combined with those of biological replicates to calculate distance ratios used to quantitatively compare relative distance between the FITC-labeled donor on the CR3 receptor and the ORB acceptor in the cell membrane between experimental conditions. *, $p < 0.01$ *versus* untreated or Fgn alone; **, $p < 0.01$ between treatment conditions.

distance ratios are obtained using FITC-CBRM1/5 *versus* FITC-ICRF44 suggests that upon activation there is a only a small fraction of total CR3 in the extended conformation and that a large, inactive fraction masks the decrease in FRET signal (Fig. 5*B*). With sβglu treatment we saw much more modest, although significant distance ratios with 1.11 ± 0.05 for FITC-ICRF44 in untreated neutrophils *versus* FITC-ICRF44 in sβglu-treated neutrophils and 1.24 ± 0.08 *versus* FITC-CBRM1/5 in sβglu-treated neutrophils (Fig. 5*E*). This suggests that sβglu treatment results in less extension of the extracellular domain than seen for full activation with fMLP. We also used FITC-Fgn to investigate how dual ligation would influence distance ratios. FITC-Fgn-treated neutrophils alone *versus* FITC-Fgn-treated neutrophils in the presence of fMLP produced a distance ratio of 1.35 ± 0.06, indicating significantly greater extension after fMLP stimulation. Interestingly,

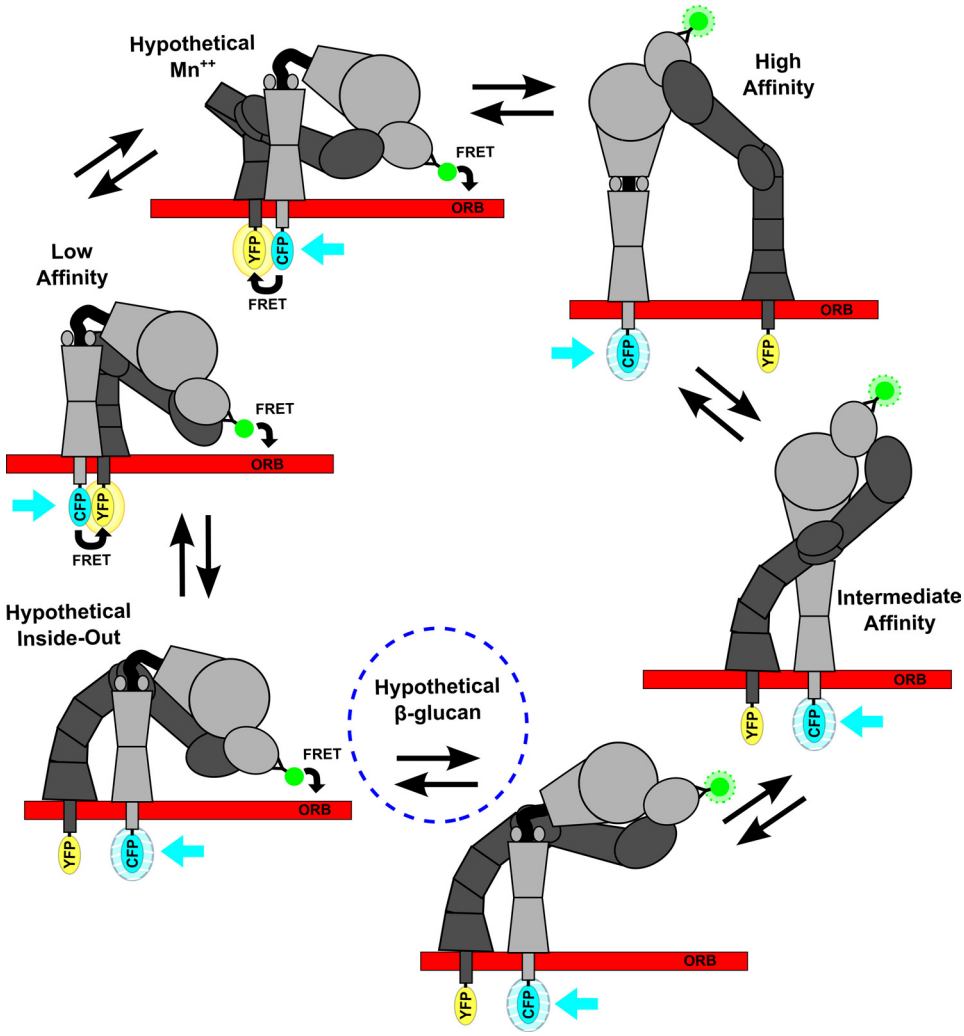


FIGURE 6. **Affinity regulation of integrins.** Electron microscopy defined low, intermediate, and high affinity conformers and hypothetical intermediates where the headpiece-tailpiece and $\alpha$ tailpiece-$\beta$ tailpiece interfaces are destabilized in outside-in or inside-out signaling. Also schematized are the predicted data in response to cytoplasmic domain and extracellular domain FRET reporter systems.

FITC-Fgn-treated neutrophils alone *versus* neutrophils treated with both FITC-Fgn and sβglu had a distance ratio of 0.93 ± 0.05, indicating a significant decrease in extension when CR3 is engaged by both Fgn and sβglu (Fig. 5*E*). Regardless of treatment condition, ORB mean fluorescence was concentration-dependent and consistent within a given experiment, demonstrating that neutrophil activation does not alter incorporation of ORB into the membrane.

*sβglu Treatment Induces Phosphorylation of Signaling Molecules and Proteins Associated with Transcriptional Regulation, mRNA Processing and Alternative Splicing*—In addition to examining the conformational changes in CR3 induced by sβglu (Fig. 6), we pursued a functional proteomics approach to identify phosphopeptides that are present in differential abundance after sβglu treatment. In these experiments K562 cell lines that were isogenic with the exception of CR3 expression were used. K563 and K562-CR3 cells with and without sβglu treatment were combined into sample groups described below, tryptic peptides were generated and enriched for phosphopeptides using TiO2 column, and the identity and abundance of the resultant peptides was interrogated using an automated nano-LC/ESI-MS analysis. To report phosphopeptide ratios, all ratios were corrected for source protein variation, and ratios of three technical replicates from an individual biological replicate were weighted on intensity and averaged. *Q*-values were calculated, and significance was set at a $q < 0.1$. The final ratio of each peptide was calculated by averaging four biological replicates.

Changes in phosphorylation level can be affected by many influences. To identify those changes specifically related to CR3 and β-glucan treatment, we identified 317 peptides representing 111 proteins and 402 unique phosphorylation sites (356 Ser(P), 43 Thr(P), and 3 Try(P)) that changed significantly in K562-CR3-treated with sβglu *versus* K562-CR3 control. From this set, a list of 53 unique phosphopeptides representing 39 proteins that changed significantly in K562-CR3 treated with sβglu *versus* K562-CR3 control but remained unchanged in K562 treated with sβglu *versus* K562 control was selected and is shown in supplemental Table S1. Functional annotation was manually curated from the Gene Ontology bioprocesses, Kyoto Encyclopedia of Genes and Genomes, and available characterization in the literature. To complement these data, we addi-

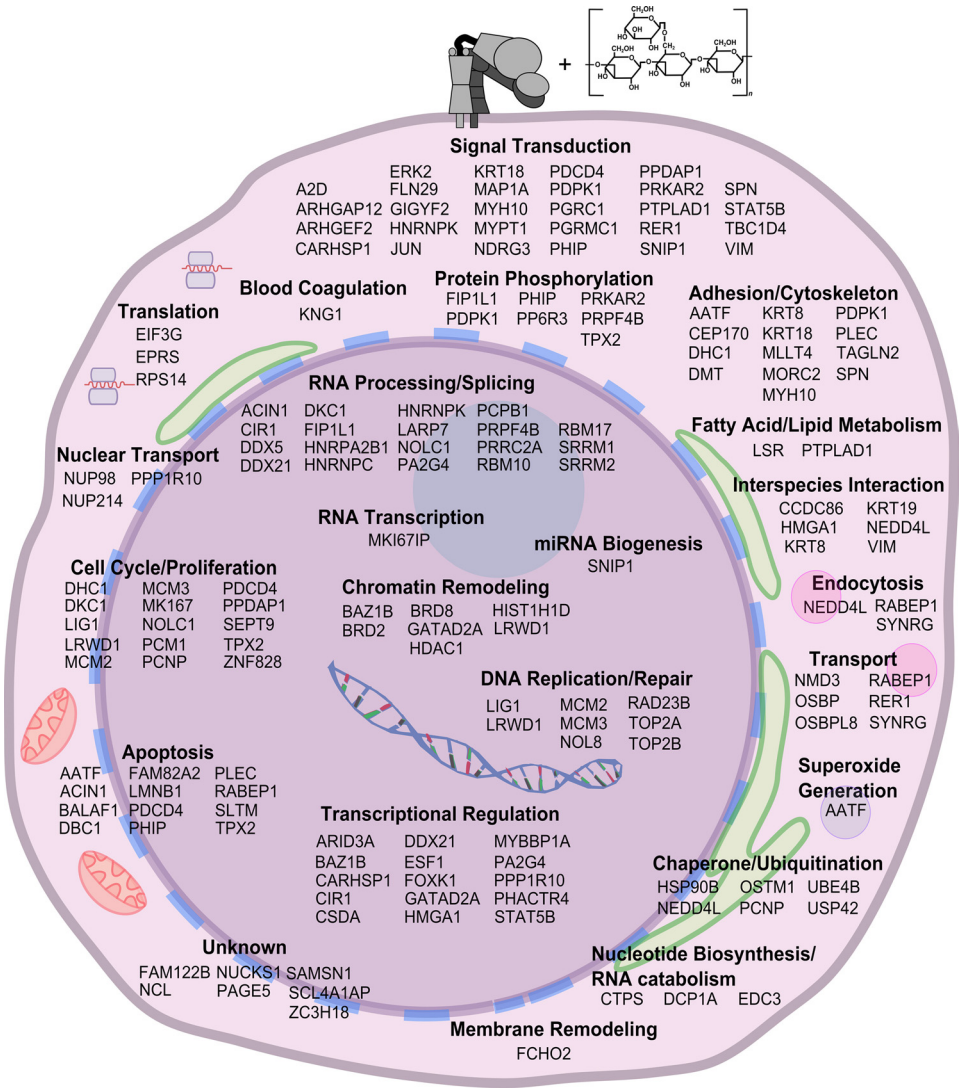


FIGURE 7. **Set of phosphopeptides differentially regulated in response to sβglu in a CR3-dependent manner.** Schematic of the phosphopeptides found using SILAC in K562 and K562:CR3 cells to be differentially regulated in response to sβglu in a CR3-dependent manner, organized by their likely cellular functions. See also supplemental Tables S1 and S2 and Fig. S3.

tionally identified 346 peptides representing 110 proteins and 441 unique phosphorylation sites (380 Ser(P), 54 Thr(P), and 7 Tyr(P)) that changed significantly in K562-CR3 treated with sβglu *versus* K562 treated with sβglu. From this set a list of 131 unique phosphopeptides representing 94 proteins was generated that changed significantly in K562-CR3 treated with sβglu *versus* K562 treated with sβglu but remained unchanged in K562-CR3 control *versus* K562 control and is shown in supplemental Table S2. Many of the phosphorylation sites that show differential regulation are non-canonical, and therefore, antibody availability for purposes of confirmation was limiting. Western blot data generated using the commercially available phosphospecific antibody for the MAP kinase ERK1/2 (Thr-185/Tyr-187) shows a 50% reduction in phosphorylation in K562-CR3 cells upon treatment with soluble sβglu but remains unchanged in K562 cells, supporting our SILAC data (supplemental Fig. S3). These phosphopeptide sets, schematized in Fig. 7, are differentially regulated in response to sβglu in a CR3-dependent manner and identify CR3 as a signaling receptor for sβglu.

## DISCUSSION

When isolated in soluble form, β-glucan has been shown to be an effective immune potentiator and is the subject of several clinical trials for both anti-infectious and anti-cancer indications (8–12). Therapeutically, sβglu has shown an ideal clinical profile in supporting host defense without stimulating the production of cytokines, which when overproduced can result in significant morbidity and mortality (31–33). The ability to achieve cellular immune stimulation in the absence of cytokine production is a unique consequence of glucan binding to CR3, but the mechanism is poorly understood. Characterizing the physical changes in integrin conformation upon sβglu binding and understanding the signal that is transduced in response to this binding provides insight into the mechanism of sβglu as a therapeutic while also facilitating the design of targeted agonists.

FRET was used to investigate intracellular and extracellular conformational changes of the $\beta_2$ integrin, CR3, in response to sβglu and the native I-domain ligand, Fgn. This study repre-

sents the first use of FRET to study PAMP recognition in live cells.

K562 cells expressing our intracellular FRET activation reporter, K562:CR3-FRETa, showed significant loss of FRET upon FgnD binding, supporting that, as with LFA-1, CR3 activation is correlated with a spatial separation of the cytoplasmic domains (Figs. 2 and 3, and supplemental Fig. S1). Significantly reduced FRET was also shown upon treatment with sβglu (Fig. 3). K562:LFA1-FRETa cells reported no loss of FRET in response to sβglu, demonstrating this response is specific to CR3. Furthermore, although treatment with FgnD alone or in combination with sβglu also significantly reduced FRET in the CR3-FRETa construct, no additive affect was observed. These studies were carried out without $Mn^{2+}$ to compensate for homotypic clumping, which likely explains the less robust loss of FRET observed in comparison to Fgn treatments in the presence of $Mn^{2+}$. The results suggest a mechanism by which β-glucan may exhibit some of its priming effect. sβglu is not known to directly activate neutrophils through CR3 but rather is thought to initiate a primed state that leads to a faster or an enhanced response when encountering a second stimulus. This FRET readout reports only the average separation distance between the cytoplasmic tails with "active" and "inactive," each likely covering a range of integrin conformations (Fig. 6). The CR3 activation reporter cannot distinguish an integrin in its inactive bent conformation from the intermediate activation state believed to be stabilized by $Mn^{2+}$. Additionally, the FRET efficiency of each cell is actually an average of all labeled CR3 molecules on the membrane. A lower FRET efficiency means that more receptors have a separation of cytoplasmic tails but does not reflect the activation state of every single receptor. Intracellular FRET reporter data, although giving valuable insight, must be coupled with other means of investigation to give a clear picture of integrin dynamics.

To further investigate the conformational state induced by sβglu, the FRET reporting system developed by Lefort *et al.* (23) was used to examine the extension of the extracellular domain of CR3 in response to sβglu. Treatment with sβglu caused a much more modest extracellular extension than would be expected, given the degree of cytoplasmic tail separation reported. Additionally, dual ligation with Fgn and sβglu showed a smaller distance ratio than that of Fgn treatment alone, suggesting that dual ligation signals may be transduced via a distinct conformational stabilization to that of Fgn or sβglu alone (Figs. 5 and 6). The extracellular extension data for dual ligation is restricted to reporting the conformation of surface receptors. As shown in Fig. 4, CR3 ligation by Fgn with and without sβglu leads to receptor internalization (Fig. 4). To isolate the conformation of dual ligated receptor on the surface, our ORB studies used FITC-Fgn as both a ligand and FRET reporter. We speculate that dual ligation stabilizes a subset of CR3 molecules on the cell surface, whereas receptors that have transitioned to the fully extended state are rapidly internalized and cleared. It is also plausible that dual ligation may slow conversion kinetics to the fully activated state.

Ligand binding is not a constitutive property of integrins. Three distinct integrin conformations have been characterized by electron microscopy (34). In the low affinity conformation, the legs and cytoplasmic domains are in close apposition to each other and bent at the knee in an inverted V shape, allowing the head to be tucked in over the legs (Fig. 6) (25). The high affinity binding state requires a switchblade-like extension in which the integrin transitions to a fully extended conformation with an open headpiece and separation of the α and β subunits at their cytoplasmic and transmembrane leg domains (Fig. 6) (24, 34). This unbending event is linked to the outward swing of the hybrid domain and a pulldown of the C-terminal helix of the β I-like domain, which alters the geometry of the metal ion-dependent adhesion site to induce the active high affinity conformation. I-domain-containing integrins additionally require the metal ion-dependent adhesion site loops and $Mg^{2+}$ coordination of the activated β I-like domain to interact with the C-terminal α I-domain α-helix and pull downward. This action converts the α I-domain through a downward displacement of one or two turns of the helix into intermediate and high affinity forms. These global conformational changes are coupled to specific inter- and intradomain rearrangements that stabilize the high affinity states of the β I-like and α I domains in the head region to permit binding of extrinsic ligands (35). In addition to these stabilized conformational states it is thought that a range of intermediates in integrin conformation are possibly based on the inherent flexibility of hinges and joints in the protein structure (36) (Fig. 6). Because of this structural flexibility, integrins in the resting conformation are thought to exhibit "breathing," which is a small degree of unbending.

In addition to the canonical "outside-in" signaling whereby ligand binding activates an intracellular signaling pathway, integrins can also transduce "inside-out" signals. In this case, signals received by cell surface receptors (*e.g.* chemokine receptors) initiate intracellular signals that impinge on the cytoplasmic domains, causing a dramatic increase of ligand affinity in the extracellular domain and possibly passing through intermediate affinity conformations (34) (Fig. 6).

The previously described integrin breathing coupled with a relaxation of leg restraints, which may result from the binding of adaptor molecules, such as talin, to the cytoplasmic tail regions in response to intracellular signaling, may allow further unbending and small outward movement of the hybrid domain sufficient to expose the epitopes of activation-specific or stimulatory antibodies (37). Fig. 6 schematizes some of these defined and hypothetical intermediate integrin conformations paired with their predicted state FRET-based readout. Our observed separation of cytoplasmic tails combined with only a modest increase in distance ratio after sβglu treatment lends support to the existence of this hypothesized intermediate conformation. Perhaps binding by sβglu occurs in small amounts, facilitated by the breathing of the integrin, which then transduces that signal via an inside-out mechanism to allow separation of cytoplasmic tails and a relaxation of the leg regions. This hypothesized conformation may structurally define the "primed state" induced by sβglu.

In addition to changes in conformation induced by sβglu, we were also interested in identifying CR3-dependent signaling responses to sβglu. The β-glucan-dependent signaling events are not well characterized, and study results are further complicated, as different sources of β-glucan may mediate their

effects through different signaling pathways (38–41). Protein-tyrosine kinase inhibitors genistein or herbimycin A were shown to significantly block CR3-dependent cytotoxicity induced by sβglu (13). Li *et al.* (11) demonstrated that the tyrosine kinase Syk was phosphorylated by mimicking dual ligation with macrophage-processed β-glucan and anti-I domain antibodies and additionally that phospho-Syk could be immunoprecipitated with CR3. Dual ligation also activated PI3K, which was shown using specific inhibitors to be downstream of Syk phosphorylation (11). In our studies, using K562 cell lines that were isogenic with the exception of CR3 expression for SILAC-coupled MS experiments allowed the generation of a sβglu phosphopeptide map that is CR3-dependent. This technique is very robust and avoids some of the run variation and derivitization artifacts seen in other proteomic techniques. Phosphopeptides whose ratios varied in a CR3-dependent and sβglu-mediated way include previously reported integrin-associated proteins, such as Vimentin, phosphatidylinositol 3-dependent protein kinase-1, STAT5B, Rho GTPase-activating protein 12, keritins 8 and 18, *N*-myc downstream regulated gene family member 3, scaffold attachment factor B-like transcription modulator, myosin heavy chain 10, sialophorin, and components of EGF signaling (42–48). Also represented were peptides known to be involved in the cellular response to other PAMPs, including ERK2 and TRAF (TNF receptor-associated factor)-type zinc finger domain-containing protein 1, the former of which was confirmed by Western blot analysis (26, 30) (supplemental Fig. S3). Additionally, the overall phosphopeptide profile was heavily weighted toward signaling molecules and proteins involved in transcriptional regulation, mRNA processing, and alternative splicing. This suggests that sβglu may exert its priming effects by altering the transcriptional state of the cell.

This global phosphoproteome is the first direct demonstration of CR3-dependent signal transduction in response to unprocessed sβglu in human cells and demonstrates that CR3 is a functional pattern recognition receptor for fungal β-glucan. The phosphopeptide signature and conformational intermediate described here may define the sβglu-primed state in human neutrophils. This work underscores the potential therapeutic value of CR3 as a target for the development of carbohydrate-based immune modulators.

*Acknowledgment—We thank Dr. Brian LeBlanc for constructive discussion and technical assistance.*

## REFERENCES


1. Xia, Y., and Ross, G. D. (1999) Generation of recombinant fragments of CD11b expressing the functional β-glucan-binding lectin site of CR3 (CD11b/CD18). *J. Immunol.* **162,** 7285–7293
2. Phaff, H. J. (1963) Cell wall of yeasts. *Annu. Rev. Microbiol.* **17,** 15–30
3. Lavigne, L. M., O'Brien, X. M., Kim, M., Janowski, J. W., Albina, J. E., and Reichner, J. S. (2007) Integrin engagement mediates the human polymorphonuclear leukocyte response to a fungal pathogen-associated molecular pattern. *J. Immunol.* **178,** 7276–7282
4. Harler, M. B., Wakshull, E., Filardo, E. J., Albina, J. E., and Reichner, J. S. (1999) Promotion of neutrophil chemotaxis through differential regulation of β1 and β2 integrins. *J. Immunol.* **162,** 6792–6799
5. Gelderman, K. A., Tomlinson, S., Ross, G. D., and Gorter, A. (2004) Complement function in mAb-mediated cancer immunotherapy. *Trends Immunol.* **25,** 158–164
6. Yauch, R. L., Berditchevski, F., Harler, M. B., Reichner, J., and Hemler, M. E. (1998) Highly stoichiometric, stable, and specific association of integrin α3β1 with CD151 provides a major link to phosphatidylinositol 4-kinase and may regulate cell migration. *Mol. Biol. Cell* **9,** 2751–2765
7. Mori, T., Ikemoto, H., Matsumura, M., Yoshida, M., Inada, K., Endo, S., Ito, A., Watanabe, S., Yamaguchi, H., Mitsuya, M., Kodama, M., Tani, T., Yokota, T., Kobayashi, T., Kambayashi, J., Nakamura, T., Masaoka, T., Teshima, H., Yoshinaga, T., Kohno, S., Hara, K., and Miyazaki, S. (1997) Evaluation of plasma (1→3)- β-D-glucan measurement by the kinetic turbidimetric limulus test, for the clinical diagnosis of mycotic infections. *Eur. J. Clin. Chem. Clin. Biochem.* **35,** 553–560
8. Hong, F., Yan, J., Baran, J. T., Allendorf, D. J., Hansen, R. D., Ostroff, G. R., Xing, P. X., Cheung, N. K., and Ross, G. D. (2004) Mechanism by which orally administered β-1,3-glucans enhance the tumoricidal activity of antitumor monoclonal antibodies in murine tumor models. *J. Immunol.* **173,** 797–806
9. LeBlanc, B. W., Albina, J. E., and Reichner, J. S. (2006) The effect of PGG-β-glucan on neutrophil chemotaxis *in vivo*. *J. Leukoc. Biol.* **79,** 667–675
10. Dellinger, E. P., Babineau, T. J., Bleicher, P., Kaiser, A. B., Seibert, G. B., Postier, R. G., Vogel, S. B., Norman, J., Kaufman, D., Galandiuk, S., and Condon, R. E. (1999) Effect of PGG-glucan on the rate of serious postoperative infection or death observed after high risk gastrointestinal operations. Betafectin gastrointestinal study group. *Arch. Surg.* **134,** 977–983
11. Li, B., Allendorf, D. J., Hansen, R., Marroquin, J., Ding, C., Cramer, D. E., and Yan, J. (2006) Yeast β-glucan amplifies phagocyte killing of iC3b-opsonized tumor cells via complement receptor 3-Syk-phosphatidylinositol 3-kinase pathway. *J. Immunol.* **177,** 1661–1669
12. Qi, C., Cai, Y., Gunn, L., Ding, C., Li, B., Kloecker, G., Qian, K., Vasilakos, J., Saijo, S., Iwakura, Y., Yannelli, J. R., and Yan, J. (2011) Differential pathways regulating innate and adaptive antitumor immune responses by particulate and soluble yeast-derived β-glucans. *Blood* **117,** 6825–6836
13. Vetvicka, V., Thornton, B. P., and Ross, G. D. (1996) Soluble β-glucan polysaccharide binding to the lectin site of neutrophil or natural killer cell complement receptor type 3 (CD11b/CD18) generates a primed state of the receptor capable of mediating cytotoxicity of iC3b-opsonized target cells. *J. Clin. Invest.* **98,** 50–61
14. Mueller, A., Raptis, J., Rice, P. J., Kalbfleisch, J. H., Stout, R. D., Ensley, H. E., Browder, W., and Williams, D. L. (2000) The influence of glucan polymer structure and solution conformation on binding to (1→3)-β-D-glucan receptors in a human monocyte-like cell line. *Glycobiology* **10,** 339–346
15. Zimmerman, J. W., Lindermuth, J., Fish, P. A., Palace, G. P., Stevenson, T. T., and DeMong, D. E. (1998) A novel carbohydrate-glycosphingolipid interaction between a β-(1–3)-glucan immunomodulator, PGG-glucan, and lactosylceramide of human leukocytes. *J. Biol. Chem.* **273,** 22014–22020
16. Kougias, P., Wei, D., Rice, P. J., Ensley, H. E., Kalbfleisch, J., Williams, D. L., and Browder, I. W. (2001) Normal human fibroblasts express pattern recognition receptors for fungal (1→3)- β-D-glucans. *Infect. Immun.* **69,** 3933–3938
17. Czop, J. K., and Kay, J. (1991) Isolation and characterization of β-glucan receptors on human mononuclear phagocytes. *J. Exp. Med.* **173,** 1511–1520
18. Goodridge, H. S., Reyes, C. N., Becker, C. A., Katsumoto, T. R., Ma, J., Wolf, A. J., Bose, N., Chan, A. S., Magee, A. S., Danielson, M. E., Weiss, A., Vasilakos, J. P., and Underhill, D. M. (2011) Activation of the innate immune receptor Dectin-1 upon formation of a phagocytic synapse. *Nature* **472,** 471–475
19. van Bruggen, R., Drewniak, A., Jansen, M., van Houdt, M., Roos, D., Chapel, H., Verhoeven, A. J., and Kuijpers, T. W. (2009) Complement receptor 3, not Dectin-1, is the major receptor on human neutrophils for β-glucan-bearing particles. *Mol. Immunol.* **47,** 575–581
20. Lavigne, L. M., Albina, J. E., and Reichner, J. S. (2006) β-Glucan is a fungal determinant for adhesion-dependent human neutrophil functions. *J. Immunol.* **177,** 8667–8675
21. Liu, J., Gunn, L., Hansen, R., and Yan, J. (2009) Combined yeast-derived β-glucan with anti-tumor monoclonal antibody for cancer immunotherapy. *Exp. Mol. Pathol.* **86,** 208–214

22. Xiong, Y. M., Chen, J., and Zhang, L. (2003) Modulation of CD11b/CD18 adhesive activity by its extracellular, membrane-proximal regions. *J. Immunol.* **171,** 1042–1050
23. Lefort, C. T., Hyun, Y. M., Schultz, J. B., Law, F. Y., Waugh, R. E., Knauf, P. A., and Kim, M. (2009) Outside-in signal transmission by conformational changes in integrin Mac-1. *J. Immunol.* **183,** 6460–6468
24. Kim, M., Carman, C. V., and Springer, T. A. (2003) Bidirectional transmembrane signaling by cytoplasmic domain separation in integrins. *Science* **301,** 1720–1725
25. Shimaoka, M., and Springer, T. A. (2003) Therapeutic antagonists and conformational regulation of integrin function. *Nat. Rev. Drug Discov.* **2,** 703–716
26. Akira, S., and Takeda, K. (2004) Toll-like receptor signaling. *Nat. Rev. Immunol.* **4,** 499–511
27. Yakubenko, V. P., Solovjov, D. A., Zhang, L., Yee, V. C., Plow, E. F., and Ugarova, T. P. (2001) Identification of the binding site for fibrinogen recognition peptide γ383–395 within the α(M)I-domain of integrin α(M)β2. *J. Biol. Chem.* **276,** 13995–14003
28. Zhang, L., and Plow, E. F. (1999) Amino acid sequences within the α subunit of integrin αMβ2 (Mac-1) critical for specific recognition of C3bi. *Biochemistry* **38,** 8064–8071
29. Diamond, M. S., Garcia-Aguilar, J., Bickford, J. K., Corbi, A. L., and Springer, T. A. (1993) The I domain is a major recognition site on the leukocyte integrin Mac-1 (CD11b/CD18) for four distinct adhesion ligands. *J. Cell Biol.* **120,** 1031–1043
30. Sanada, T., Takaesu, G., Mashima, R., Yoshida, R., Kobayashi, T., and Yoshimura, A. (2008) FLN29 deficiency reveals its negative regulatory role in the Toll-like receptor (TLR) and retinoic acid-inducible gene I (RIG-I)-like helicase signaling pathway. *J. Biol. Chem.* **283,** 33858–33864
31. Osuchowski, M. F., Welch, K., Yang, H., Siddiqui, J., and Remick, D. G. (2007) Chronic sepsis mortality characterized by an individualized inflammatory response. *J. Immunol.* **179,** 623–630
32. Babineau, T. J., Hackford, A., Kenler, A., Bistrian, B., Forse, R. A., Fairchild, P. G., Heard, S., Keroack, M., Caushaj, P., and Benotti, P. (1994) A phase II multicenter, double-blind, randomized, placebo-controlled study of three dosages of an immunomodulator (PGG-glucan) in high-risk surgical patients. *Arch. Surg.* **129,** 1204–1210
33. Babineau, T. J., Marcello, P., Swails, W., Kenler, A., Bistrian, B., and Forse, R. A. (1994) Randomized phase I/II trial of a macrophage-specific immunomodulator (PGG-glucan) in high risk surgical patients. *Ann. Surg* **220,** 601–609
34. Takagi, J., Petre, B. M., Walz, T., and Springer, T. A. (2002) Global conformational rearrangements in integrin extracellular domains in outside-in and inside-out signaling. *Cell* **110,** 599–611
35. Shimaoka, M., Xiao, T., Liu, J. H., Yang, Y., Dong, Y., Jun, C. D., McCormack, A., Zhang, R., Joachimiak, A., Takagi, J., Wang, J. H., and Springer, T. A. (2003) Structures of the αLI domain and its complex with ICAM-1 reveal a shape-shifting pathway for integrin regulation. *Cell* **112,** 99–111
36. Mould, A. P., and Humphries, M. J. (2004) Regulation of integrin function through conformational complexity. Not simply a knee-jerk reaction? *Curr. Opin. Cell Biol.* **16,** 544–551
37. Askari, J. A., Buckley, P. A., Mould, A. P., and Humphries, M. J. (2009) Linking integrin conformation to function. *J. Cell Sci.* **122,** 165–170
38. Nakamura, K., Kinjo, T., Saijo, S., Miyazato, A., Adachi, Y., Ohno, N., Fujita, J., Kaku, M., Iwakura, Y., and Kawakami, K. (2007) Dectin-1 is not required for the host defense to *Cryptococcus neoformans*. *Microbiol. Immunol.* **51,** 1115–1119
39. Saijo, S., Fujikado, N., Furuta, T., Chung, S. H., Kotaki, H., Seki, K., Sudo, K., Akira, S., Adachi, Y., Ohno, N., Kinjo, T., Nakamura, K., Kawakami, K., and Iwakura, Y. (2007) Dectin-1 is required for host defense against *Pneumocystis carinii* but not against *Candida albicans*. *Nat. Immunol.* **8,** 39–46
40. Taylor, P. R., Tsoni, S. V., Willment, J. A., Dennehy, K. M., Rosas, M., Findon, H., Haynes, K., Steele, C., Botto, M., Gordon, S., and Brown, G. D. (2007) Dectin-1 is required for β-glucan recognition and control of fungal infection. *Nat. Immunol.* **8,** 31–38
41. LeibundGut-Landmann, S., Gross, O., Robinson, M. J., Osorio, F., Slack, E. C., Tsoni, S. V., Schweighoffer, E., Tybulewicz, V., Brown, G. D., Ruland, J., and Reis e Sousa, C. (2007) Syk- and CARD9-dependent coupling of innate immunity to the induction of T helper cells that produce interleukin 17. *Nat. Immunol.* **8,** 630–638
42. Khunkaewla, P., Schiller, H. B., Paster, W., Leksa, V., Cermák, L., Andera, L., Horejsí, V., and Stockinger, H. (2008) LFA-1-mediated leukocyte adhesion regulated by interaction of CD43 with LFA-1 and CD147. *Mol. Immunol.* **45,** 1703–1711
43. Trucy, M., Barbat, C., Fischer, A., and Mazerolles, F. (2006) CD4 ligation induces activation of protein kinase Cζ and phosphoinositide-dependent-protein kinase-1, two kinases required for down-regulation of LFA-1-mediated adhesion. *Cell Immunol.* **244,** 33–42
44. Defilippi, P., Venturino, M., Gulino, D., Duperray, A., Boquet, P., Fiorentini, C., Volpe, G., Palmieri, M., Silengo, L., and Tarone, G. (1997) Dissection of pathways implicated in integrin-mediated actin cytoskeleton assembly. Involvement of protein kinase C, Rho GTPase, and tyrosine phosphorylation. *J. Biol. Chem.* **272,** 21726–21734
45. Alam, H., Kundu, S. T., Dalal, S. N., and Vaidya, M. M. (2011) Loss of keratins 8 and 18 leads to alterations in α6β4-integrin-mediated signaling and decreased neoplastic progression in an oral tumor-derived cell line. *J. Cell Sci.* **124,** 2096–2106
46. Bernaciak, T. M., Zareno, J., Parsons, J. T., and Silva, C. M. (2009) A novel role for signal transducer and activator of transcription 5b (STAT5b) in β1-integrin-mediated human breast cancer cell migration. *Breast Cancer Res.* **11,** R52
47. Tuck, A. B., Elliott, B. E., Hota, C., Tremblay, E., and Chambers, A. F. (2000) Osteopontin-induced, integrin-dependent migration of human mammary epithelial cells involves activation of the hepatocyte growth factor receptor (Met). *J. Cell Biochem.* **78,** 465–475
48. Cabodi, S., Morello, V., Masi, A., Cicchi, R., Broggio, C., Distefano, P., Brunelli, E., Silengo, L., Pavone, F., Arcangeli, A., Turco, E., Tarone, G., Moro, L., and Defilippi, P. (2009) Convergence of integrins and EGF receptor signaling via PI3K/Akt/FoxO pathway in early gene Egr-1 expression. *J. Cell Physiol.* **218,** 294–303